

# Underwater radiated noise from small vessels in shallow water: propagation modelling and experimental measurements

T A Smith, PhD, CEng, MRINA<sup>a\*</sup>, M Kourouniotti, BEng, AMRINA<sup>a</sup>,

<sup>a</sup>Marine Research Group, Dept. Mechanical Engineering, University College London, United Kingdom;

\*Corresponding author. Email: tom.smith.17@ucl.ac.uk

## Synopsis

Underwater noise is a growing problem in many of the world's oceans and waterways, with a large body of research now showing the detrimental impact this has on marine life. Noise in shallow coastal waters is a particular problem because the concentration of both marine life and human activity is often much higher. Furthermore, noise attenuates more slowly in shallow water, and so its impact is greater. For naval operations, this can increase the detection distance of a vessel, which places more onerous requirements on the designer to reduce the levels of radiated noise, and potentially degrades the operability of the vessel when operating in shallow littoral waters. In this work, the impact of small vessels on the levels of underwater noise in a shallow water environment is considered. Acoustic recordings are obtained using a hydrophone and the data are analysed to determine the sound levels and frequency content from different vessels. The noise levels recorded are found to greatly exceed those caused by environmental factors and occur primarily over the frequency range  $63 \leq f \leq 500$  Hz, unless propeller singing or cavitation are present, in which case excess noise levels can occur for frequencies up to 20 kHz. Over a 25-minute period, the mean overall sound pressure level is found to be in excess of 90 dB, which is attributed to only a small number of boats operating in the test area. To provide more insight into noise propagation in shallow water, numerical modelling is carried out by numerically solving the acoustic wave equation in the time domain, which allows for phenomena such as reflection, absorption, and wave interactions to be captured. Propagation of sound from a source located at the sea surface is computed for deep and shallow water, with two different seabed materials also being considered. The propagation pattern in shallow water is shown to be more complex than for deep water, with the reflection/absorption properties of the seabed playing an important role along with the depth.

*Keywords:* Underwater radiated noise, marine environment, computational acoustics

## 1 Introduction

Underwater noise resulting from human activity is a growing problem with increasing numbers and sizes of vessels contributing to a significant rise in the ambient noise levels in seas, oceans, and waterways around the world. These noise levels are having a detrimental impact on many marine ecosystems, leading to growing calls for better regulation and legislation of marine activities with regards to the noise produced. For naval operations, the importance of underwater noise as a means of detecting vessels has long been understood. This has led to continuous development in sonar and hydrophone technology, matched by a continual need to reduce the radiated noise from both surface vessels and submarines.

Over the past couple of decades, a large body of evidence has built up showing the negative impacts of anthropogenic noise from shipping and other marine traffic on marine life. This includes cetaceans (Nowacek et al., 2007; Dyndo et al., 2015; Wisniewska et al., 2018), and many species of fish and invertebrates (Simpson et al., 2016; Mickle and Higgs, 2018; Murchy et al., 2019). Alongside this, numerous studies have been conducted to determine the radiated noise levels from commercial and other vessels: both to investigate the noise produced by specific vessels (Arveson and Vendittis, 2000; McKenna et al., 2012; Li et al., 2018) and also to measure and monitor noise levels from shipping in a particular area (Farcas et al., 2020; Lalander et al., 2021; Putland et al., 2022). Despite much of the focus in recent years being on the impact of large commercial vessels, recent evidence has suggested that small vessels could be contributing more to the overall soundscape than previously acknowledged, particularly in shallow coastal waters (Erbe et al., 2016; Hermannsen et al., 2019; Cope et al., 2021). These studies have highlighted the need to better understand the levels of noise from small vessels and the impact this is having on marine life in the areas where they operate.

Shallow coastal waters present a particular challenge for operational, geographical, naval and ecological reasons. Firstly, many such areas have a high concentration of marine traffic due to vessels entering and leaving ports and harbours, ferries, and recreational vessels which mostly operate close to shore. Secondly, shallow coastal waters are home to a large percentage of marine biodiversity, including marine mammals, birds, fish, and invertebrates.

---

### Authors' Biographies

**Dr. Tom Smith** is a senior research fellow in naval architecture at University College London. He has a PhD in Mechanical Engineering and is a chartered engineer. His research focuses on fluid-induced noise, underwater radiated noise and marine hydrodynamics.

**Margarita Kourouniotti** is a post-graduate student at UCL, studying for an MSc in Marine Engineering. She has interests in underwater noise, cavitation, and experimental acoustics.

This means that noise produced in such waters is having a larger impact than the same noise produced in the open ocean. Finally, noise attenuates more slowly in shallow water than it does in deep water (Ainslie et al., 2014). Thus, for a given source intensity, the sound pressure level at some distance away will be greater in shallow water as compared to deep water.

Human impact on ecosystems and wildlife is coming into much sharper focus outside of academic communities, and this is increasing the pressure on governments and other bodies to reduce the impact our actions have on the natural world. During the lockdowns imposed during the COVID pandemic, there were many reports in local and national media of animals being sighted in places they would not normally be found, or in larger numbers. There were multiple reports of seals much further up the Thames<sup>1</sup> and also in parts of the Solent<sup>2</sup> where they are rarely seen. Seals are known to be very sensitive to human activity with several studies showing that seals avoid noisy marine environments (Halliday et al., 2020). As well as highlighting the impact we are having on these habitats, this also shows us that wildlife can adapt and recover quickly if given the chance.

Shallow water presents a number of challenges for naval operations from a signatures perspective. For a vessel seeking to avoid detection, the reduced attenuation increases the detection distance. For mine counter-measure operations, this represents a particular challenge that needs to be considered to protect assets (either manned or unmanned) operating in what is already a difficult environment. On the other hand, for vessels tasked with tracking other vessels, the multiple reflections off the seabed and sea surface, combined with variable seabed properties and bathymetry make localising acoustic sources more challenging.

Regulations and legislation on underwater noise from human activities is very limited at present, particularly for smaller vessels. Many classification societies have “quiet ship” notations, but such notations are primarily for larger commercial or research vessels and cannot be readily applied to small recreational boats. There are currently no international regulations limiting the noise produced by smaller vessels, and underwater radiated noise is rarely prioritised by designers and builders. Much of this stems from a lack of data showing what the noise levels are and what impact this has, as well as a lack of economic incentives to make improvements. Despite increased interest in measuring noise levels from specific vessels and specific areas of water, the lack of data remains a major obstacle, both in terms of bringing in new legislation and also to designers and boat and ship builders who need to reduce the noise their vessels produce.

Some coastal waterways such as river estuaries and harbours have speed restrictions in place for safety reasons and to reduce erosion, and there is evidence that these can also be effective at reducing noise levels (MacGillivray et al., 2019) particularly if the reduced speed eliminates cavitation. Many trials have shown that a positive relationship exists between speed and radiated noise levels for large ships, but the relationship is seldom linear due to changes in propeller loading, the emergence of cavitation, propeller singing, and other phenomena. Furthermore, a number of studies have shown that vessels can produce more noise at lower speeds than higher speeds. This can occur for a variety of reasons. For example in one study (Svedendahl et al., 2021), it was found that one of the boats tested produced more noise at 9 knots than at 18 knots. Underwater cameras revealed that this was due to the cavitation being worse at 9 knots, and it was noted that the propeller was designed for speeds above 20 knots. For vessels fitted with controllable-pitch propellers (CPP), reducing speed through a pitch-reduction rather than a shaft speed reduction can also lead to increased noise levels (Tani et al., 2015). Reducing propeller pitch at constant shaft speed can lead to significant levels of pressure-side cavitation as well as other types of cavitation due to the propeller operating in an off-design condition. Thus, the effectiveness of speed restrictions will depend on the type of vessel and its propulsion architecture, and further research is needed to provide a more complete understanding of how speed and noise relate on a broader range of vessels. Given the prevalence of CPPs on many naval vessels, this needs to be given particular attention as it means that the cavitation inception speed will depend on the mode of operation.

In this study, the contribution of small vessels to underwater noise levels in shallow water is considered together with an investigation into shallow water noise propagation. Section 2 presents a discussion on noise propagation in shallow water, with acoustic simulations used to illustrate the influence of water depth on propagation losses and overall noise levels. Section 3 presents the results of a trial carried out in the Solent, off the south coast of England, where a hydrophone was used to record noise levels at a particular location. This has allowed for the noise levels and frequency content of different types of vessel to be examined, including small fishing vessels, motor yachts and rigid inflatable boats (RIBS). Changes in noise levels with speed are considered and the signatures from different

---

<sup>1</sup>[www.thamesestuarypartnership.org](http://www.thamesestuarypartnership.org)

<sup>2</sup>[www.advertiserandtimes.co.uk](http://www.advertiserandtimes.co.uk)

vessels are analysed to identify the dominant noise sources and to determine the excess noise levels from small vessels ( $\leq 20\text{m}$ ) operating in shallow coastal waters.

## 2 Sound propagation in shallow water

As well as the intensity of the acoustic source, the propagation of the acoustic waves over a given distance plays an important role in determining the overall noise levels in a particular part of the ocean. The lower the propagation losses, the higher the noise levels will be for a fixed set of acoustic sources. Propagation losses, PL, in water are commonly modelled using the following equation:

$$\text{PL} = A \log_{10}(R) \quad (1)$$

where  $R$  denotes the distance from the source to the receiver and  $A$  is some constant depending on the conditions, in particular the depth. In deep water, noise is often assumed to spread spherically over short to medium distances, leading to  $A = 20$  and hence a propagation loss of 6 dB per doubling of distance from the source. This approach is acknowledged by the ITTC in their guidelines for full-scale measurements of underwater radiated noise from ships (ITTC, 2017), and is also proposed by American Bureau of Shipping (ABS) and Lloyd's Register in the absence of transmission loss modelling based on trials at multiple distances. Some classification societies have adopted slightly different values, for example  $A = 18$  by Det Norske Veritas (DNV) and  $A = 19$  by Bureau Veritas (BV).

In shallow water, the propagation loss is more complex due to the effects of the seabed and sea surface (Tielburger et al., 1997; Ainslie et al., 2014), but is lower than that in deep water. In the context of the above modelling, it is often said that the propagation is generally closer to either cylindrical spreading where  $A = 10$ , or mode-stripping, which lies somewhere between spherical and cylindrical spreading depending on the water depth, frequency and source depth (Weston, 1971). Cylindrical spreading leads to a loss of 3 dB per doubling of distance as oppose to 6 dB in the case of spherical spreading.

To better understand how acoustic waves propagate in shallow water, a series of simulations have been conducted. These simulations utilise the acoustic wave equation, which is solved on a two-dimensional domain with a length of  $L = 120$  m and a variable depth,  $d$  (see figure 1). The sound source is assumed to be a monopole and is constructed by superimposing five waves over the frequency range  $125 \leq f_i \leq 500$  Hz, which is representative of the typical tonal frequencies associated with small high-speed vessels (Svedendahl et al., 2021). These frequencies, given in table 1 are chosen randomly and each wave is assigned a random phase angle to provide a more realistic scenario. Further details of the modelling are given in appendix A and in (Smith and Ventikos, 2022). To isolate the

Table 1: Acoustic waves used for propagation modelling.

Component	Amplitude (Pa)	Frequency (Hz)	Phase angle (rad)
1	1	125	0.00
2	1	180	0.24
3	1	284	1.37
4	1	376	0.67
5	1	461	2.02

effects of water depth, the water is modelled as having constant density of  $\rho_{water} = 1000\text{kgm}^{-3}$  and sound speed  $c_{water} = 1500\text{ms}^{-1}$ . The reflection/transmission of waves at the seabed is modelled by treating the seabed as a homogeneous material with a different density and sound speed to the water. Two materials are considered which are representative of a soft and hard seabed. These are taken from (Larsson and Abrahamsson, 2003) and have a speed of sound and density of  $c_{seabed} = 1700\text{ms}^{-1}$  and  $\rho_{seabed} = 1200\text{kgm}^{-3}$  for the soft seabed and  $c_{seabed} = 4000\text{ms}^{-1}$  and  $\rho_{seabed} = 2700\text{kgm}^{-3}$  for the hard seabed. Water depths of  $d = 15\text{m}$  and  $d = 30\text{m}$  are considered alongside deep water which is modelled using a physical water depth of 150m together with a perfectly matched layer (PML) to prevent wave reflections, thus creating an infinite effective depth with no bottom reflections. The equations are solved using the numerical approach set out in (Smith and Ventikos, 2022). A finite-volume approach is used with a grid resolution of approximately 30 cells per wavelength based on the shortest wave, as this was shown by Smith and Ventikos (2022) to be adequate to prevent artificial dissipation.

Because the simulations are two-dimensional, it is necessary to make a correction to the results to account for the effect of the additional dimension. If one assumes that reflected waves remain in the same plane as the respective incident waves, which is valid for a flat and smooth seabed, then the sound pressure level at a given radius  $r$

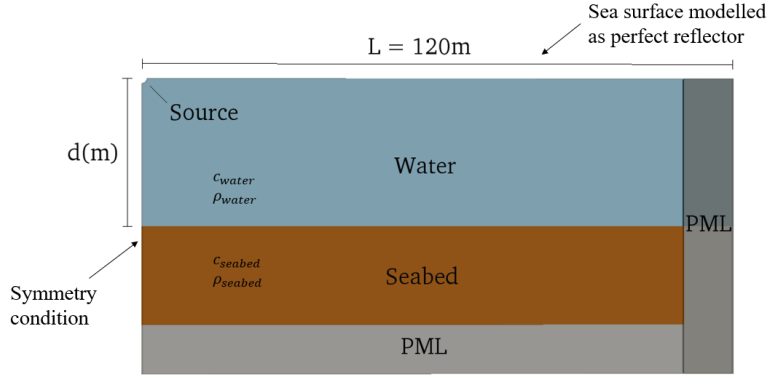


Figure 1: Domain used to model acoustic propagation through water of depth  $d$  (m). Perfectly matched layers (PML) are used to prevent unwanted wave reflections off the far-field boundaries.

from the source is

$$\text{SPL} = 20 \log_{10} \left( \frac{p_{rms}}{p_{ref}} \right) - 20 \log_{10} (\sqrt{R}) \quad (2)$$

where  $p_{rms}$  denotes the root-mean-square of the acoustic pressure obtained from the simulation. The second term on the right-hand-side accounts for the propagation loss in the third dimension. The reference pressure is  $p_{ref} = 1 \mu\text{Pa}$

Snapshots of the acoustic field for each of the five simulations are given in figure 2. For the deep water case, the expected spreading pattern is seen, with waves radiating away from the source with no interference. For the shallow water cases, the effect of the seabed is significant, with the hard seabed cases showing substantially more complex acoustic fields than the cases with a soft seabed. The initial wave reflections off the seabed can be seen in all cases, with multiple interference patterns developing for the hard seabed cases. For the soft seabed cases, it is clear that the propagation losses are greater, although for the shallowest case the attenuation appears to be lower than for the  $d=30\text{m}$  case.

To provide further insight into the propagation losses for the different cases, the overall sound pressure level has been computed for a duration equivalent to 100 time periods of the longest wave, which ensures that the results are statistically stationary. This is shown in figure 3 along a line from the source location to a point at  $x = 100\text{m}$  and  $d = 10\text{m}$ . The sound pressure level assuming spherical spreading is also shown for comparison. The deep water simulation predicts a propagation loss equivalent to spherical spreading, which demonstrates the validity of the model. The shallow water simulations show that the propagation loss depends on both the water depth and the characteristics of the sea bed. For a depth of 30m and a soft, absorbing seabed the propagation loss is very similar to that of the deep water case. This is because the seabed absorbs the majority of each acoustic wave, and the water depth means that there are only a small number of reflections between the seabed and sea surface. For a 30m depth and a hard seabed, the propagation losses are similar over the first part of the acoustic field, but differ over the latter part. This agrees with the work of Ainslie et al. (2014), who showed that the first part of the propagation will always be spherical. Over the latter part, the propagation losses are smaller and there are significant variations along the length of the domain. This is caused by the interactions between the different waves as they reflect off both the seabed and the sea surface, leading to a mean acoustic field with significant spatial variations. These variations will depend on the water depth, the seabed, and the frequency content of the acoustic source. A similar pattern is seen for the 15m case with a hard seabed, with the overall propagation loss being significantly lower than for deep water. The propagation loss in 15m deep water with a soft seabed is lower than in 30m deep water with the same seabed, indicating that at this depth the small portion of the wave that is reflected by the seabed is more significant than it was at 30m.

Further investigation into the spatial variations in the sound pressure level shows that the acoustic field is more complex than is acknowledged by typical propagation models. Figure 4 shows how the overall sound pressure level varies over the domain. Substantial variations exist for different depths, and at  $x = 100\text{m}$  the overall sound pressure level varies by up to 5.1 dB between the sea bed and sea surface. Figure 5 shows how the magnitude of each frequency component of the sound at varies with depth at  $x = 100\text{m}$ . Large variations are seen for each frequency, but no clear pattern emerges. The levels of constructive or destructive interference will depend on the

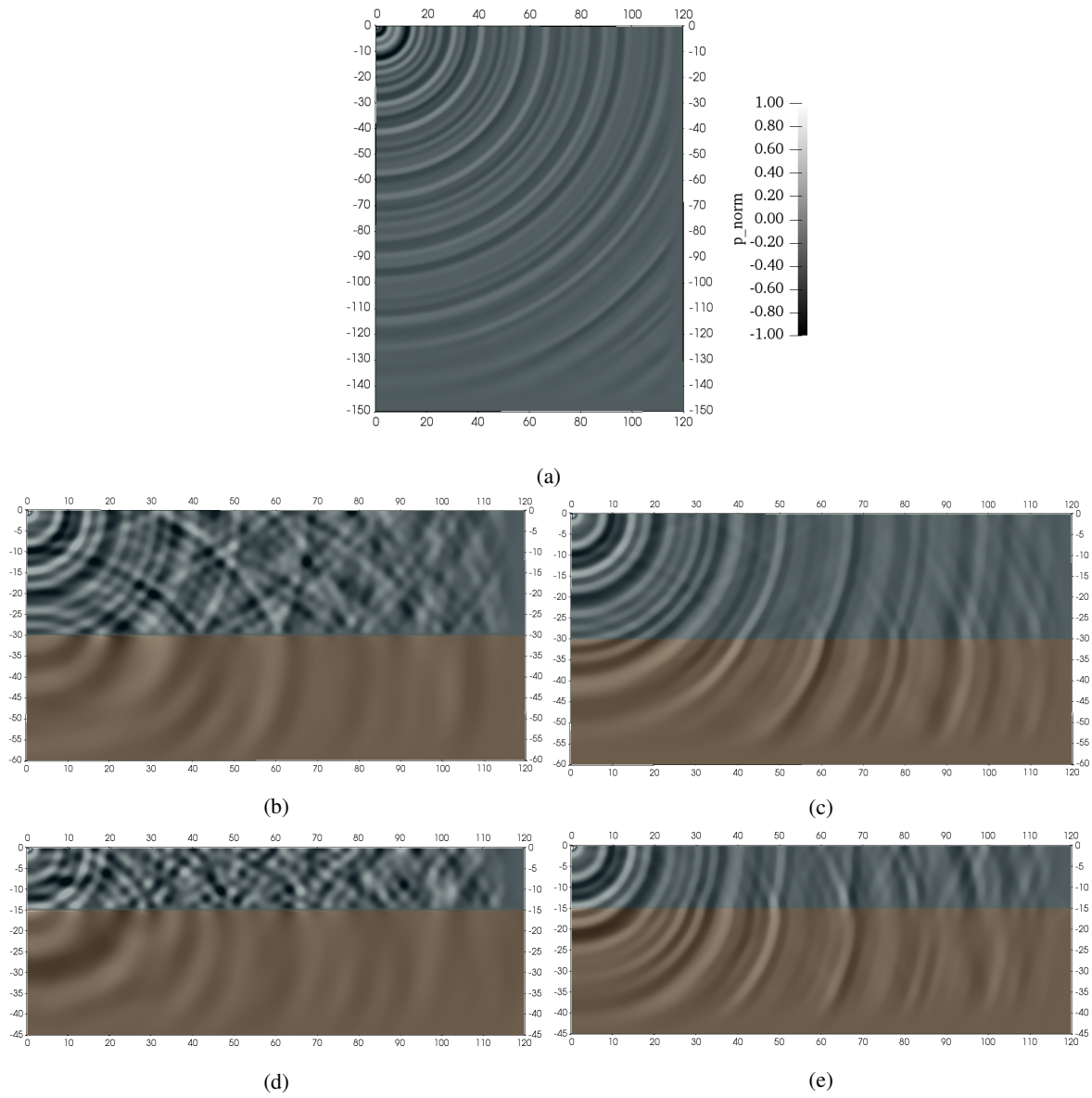


Figure 2: Snapshots of the acoustic pressure field (normalised to  $p_{norm} \in [-1, 1]$ ) for (a) deep water, (b)  $d=30\text{m}$ , hard seabed, (c)  $d=30\text{m}$ , soft seabed, (d)  $d=15\text{m}$ , hard seabed, (e)  $d=15\text{m}$ , soft seabed.

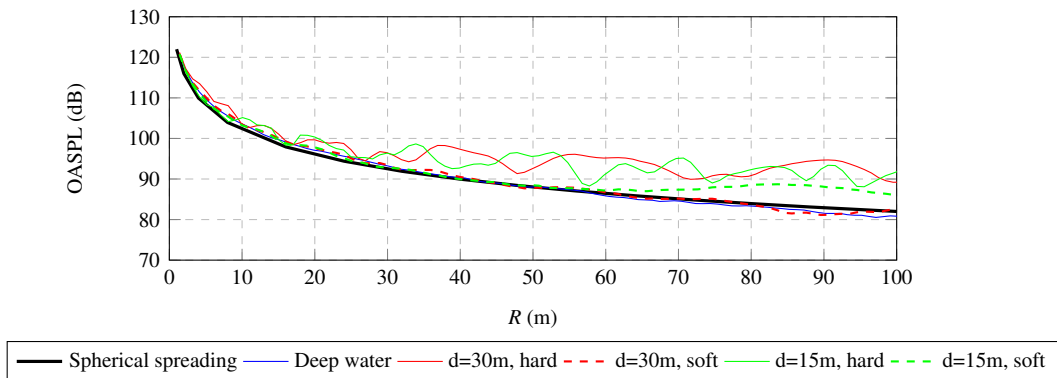


Figure 3: Sound pressure level along a line from (1,-1) to (100,-10) for each case. The reference pressure is  $p_{ref} = 1\mu\text{Pa}$ .

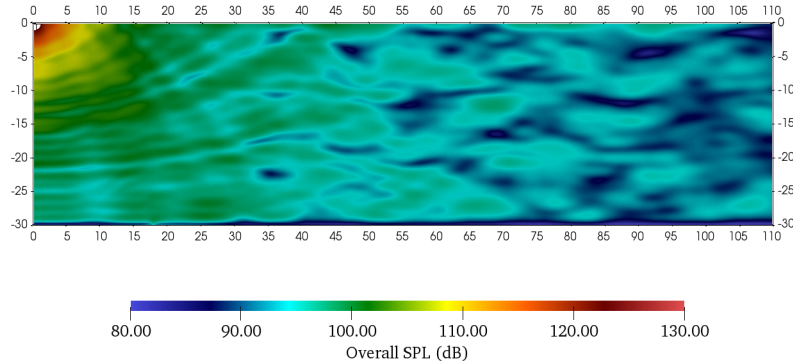


Figure 4: Overall sound pressure level for the  $d = 30\text{m}$ , hard seabed case. The sound pressure is shown for the water only and excludes the PML region.

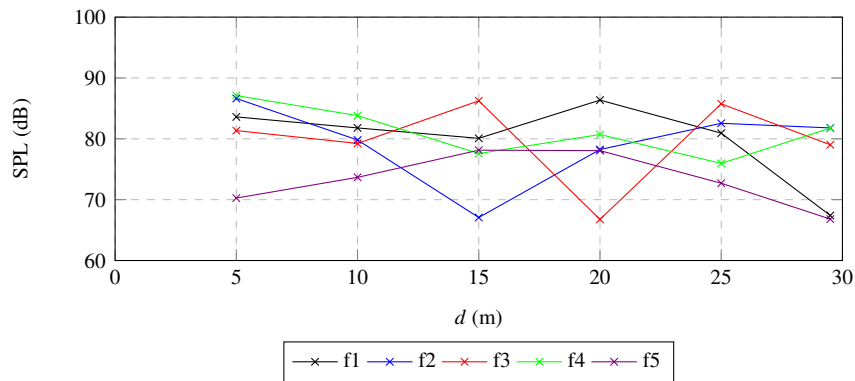


Figure 5: Sound pressure level for each of the five frequencies of the acoustic source at different depths for  $x = 100\text{m}$

relationship between the water depth and the acoustic wavelengths, and so the spatial character of the acoustic field will depend on both the source and the environment.

Aside from the increased complexity of the acoustic field, these results clearly show a reduction in the propagation loss for shallow water. The shallowest water considered  $d = 15\text{m}$  showed a reduced propagation loss for both the hard seabed and also the soft seabed, indicating that sound will decay more slowly in very shallow water even for an acoustically soft seabed. Therefore, for an acoustic source with a given strength such as a vessel travelling at a specific speed, the overall sound pressure levels in the surrounding area will be higher than they would be in deep water. The results also highlight the importance of both the water depth and the seabed material on the propagation in such environments.

### 3 Hydrophone measurements in the Western Solent

The previous section looked at how acoustic waves propagate in shallow water and showed that the propagation losses are smaller than for deep water. In this section, data are presented that provide an insight into the actual soundscape created by small vessels operating in a shallow water environment. To do this, a hydrophone was deployed in the Solent to monitor the noise levels over a period of time and to determine the acoustic characteristics of a small vessel with an outboard engine. The test area, shown in figure 6, was chosen because it is very shallow (typical depths are  $< 20\text{m}$ ) and the marine traffic is dominated by small recreational vessels. The majority of the larger commercial vessels accessing Southampton and Portsmouth harbours do so via the eastern part of the Solent and are  $\geq 10\text{ km}$  away from the test area. The trial was conducted on 29th July, 2022. The weather conditions were benign, at around Beaufort 2 and so were not thought to have negatively affected the results. The noise was recorded using a TR Porpoise hydrophone. Trials were conducted around high tide, and the hydrophone was



Figure 6: Map of the Solent area with the test area shown in red, produced using Google Maps.

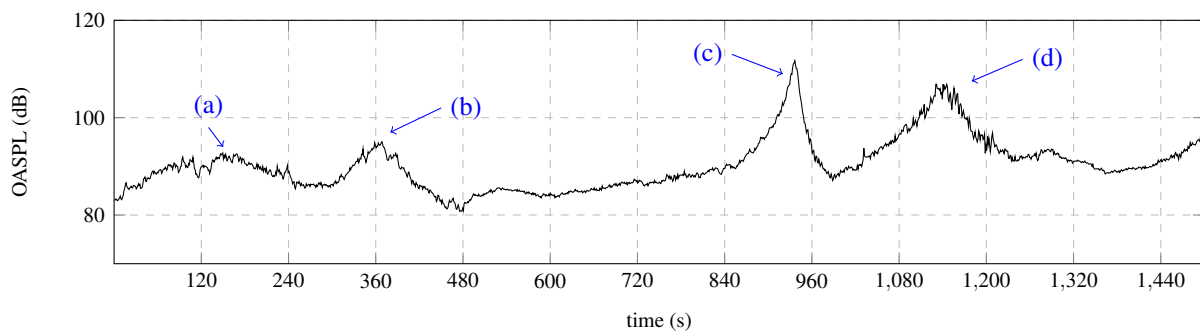


Figure 7: Overall sound pressure level recorded over a 25 minute period.

deployed 0.5m above the seabed. This is based on guidance from a number of sources, (Ainslie et al., 2021) for example, which suggest locating the hydrophone close to the bottom of the seabed to obtain more reliable results. The water depth at the hydrophone location was measured with an echo sounder and was 10 m. Data were sampled at a rate of 64 kHz. The sound pressure levels have been obtained by splitting the data into 1 second intervals with a 50% overlap and using a Hamming window. This resulted in windows containing 64000 samples, with a spectral resolution of 1 Hz.

The trial was conducted using a 5.85m rigid-inflatable boat (RIB) powered by an outboard engine. As well as recording background measurements, the acoustic signature of this vessel at multiple speeds was also recorded. The engine is a 4 cylinder 4-stroke engine with a maximum power output of 103 kW, and a maximum shaft speed of 6000 rpm. The propeller is 3-bladed and fixed pitch. The gear ratio is 1:2.59.

Much insight into the make-up of anthropogenic noise at a location can be gained from measuring sound levels for a period of time and recording the traffic in the area. Small vessels typically do not have Automatic Identification System (AIS) transceivers that broadcast speed and location and so it is necessary to estimate their speed and distance from the hydrophone. The data are not therefore used to compare one vessel to another, but instead provide a picture of what the actual noise levels are at a given location. Figure 7 shows the overall sound pressure level recorded by the hydrophone over a 25 minute period. During this time, numerous small boats, including motor yachts and a fishing boat came within 200m of the hydrophone, and in some cases closer. No large commercial vessels or ferries were within 1km of the hydrophone during this time. The overall sound pressure level during this period was  $80.8 \text{ dB} \leq \text{OASPL} \leq 111.7 \text{ dB}$ , with a mean of 91.3 dB, which is over 30 dB higher than would be expected in the absence of any marine traffic (Wenz, 1962; Thorne, 1990). The four points (a-d) correspond to a small fishing vessel operating at low speed (a), two small ( $L < 10\text{m}$ ) planing boats (b), a larger flybridge motor yacht ( $L \approx 20\text{m}$ ) travelling at high speed (c), and two motor yachts travelling in close proximity (d).

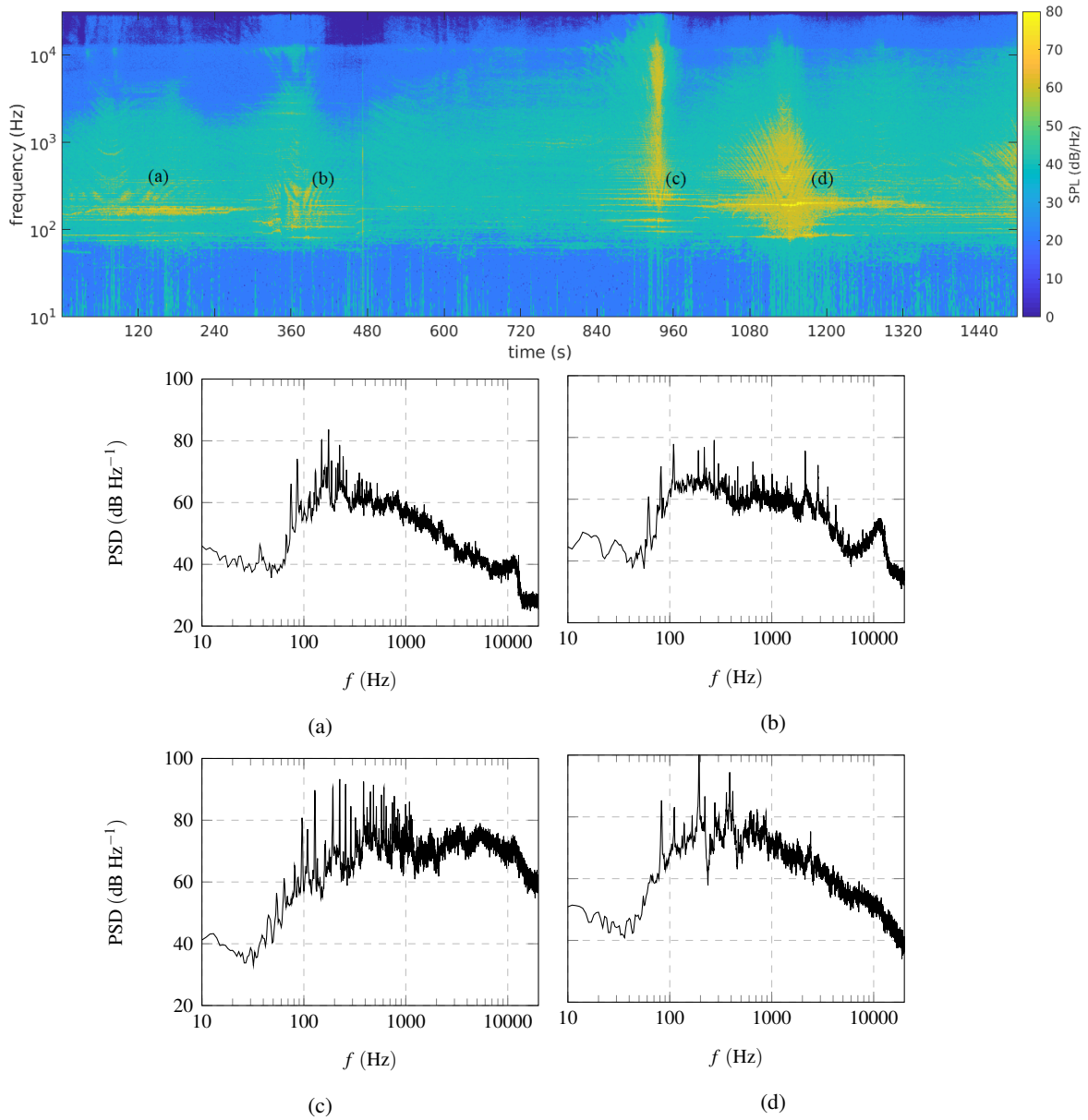


Figure 8: Spectrogram showing the sound pressure level over a 25 minute period together together with narrowband spectra for (a) fishing vessel, (b) two small planing boats, (c) flybridge yacht, and (d) two motor yachts.



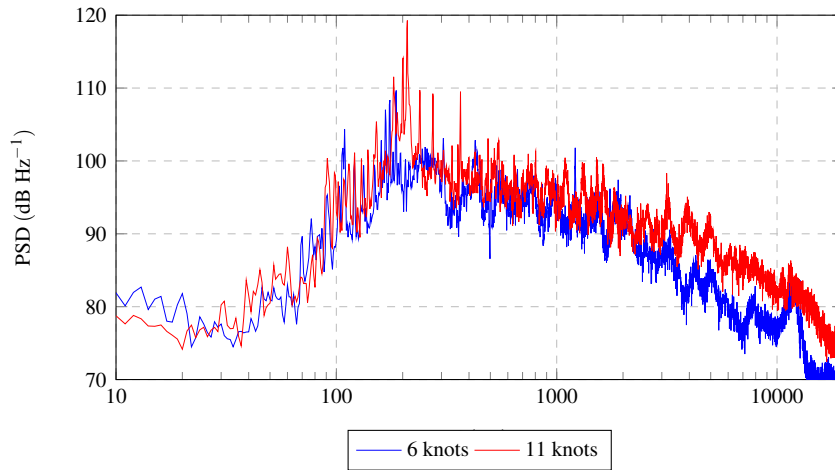


Figure 9: Sound pressure level re  $1\mu\text{Pa}$  at 1m for the RIB at 6 and 11 knots.

Figure 8 shows a spectrogram of the sound pressure level over the 25 minute period, providing additional insight into the noise levels as this shows how they are distributed across different frequencies. The elevated noise levels associated with points (a-d) in figure 7 can also be seen here. In all cases, the acoustic signatures of the vessels contain tonal components in the 63 - 500 Hz range, which correspond to a combination of the propeller blade rate and harmonics, as well as tonal components associated with the engine such as the cylinder firing rates. The signature of the fishing vessel (figure 8a) is dominated by these narrowband components, with a notable drop of in the sound pressure level at higher frequencies. There are similarities seen in the frequency content of the two small high-speed boats (figure 8b), but there is a notable difference. Beginning at 2130 Hz, there is a series of equally spaced tones, which decrease in amplitude with increasing frequency. Based on the size and frequency, this is strongly indicative of propeller singing. The signature of the flybridge yacht, as indicated by both the spectrogram and the sound pressure levels in figure 8c, indicates very developed cavitation. There are multiple high amplitude tonal components as well as a large broadband contribution at higher frequencies, which is indicative of cavitation.

As well as measuring the noise levels from passing vessels, trials were conducted to measure the acoustic signature of the RIB at 6 and 11 knots, with the hydrophone located 100m from the closest point of approach (CPA). The propagation modelling from the previous section is used to compute the 1m equivalent source levels for the data. A mean depth of 15m has been assumed and a soft seabed, which is representative of the conditions in the test area. Ambient noise levels were measured before and after each trial to ensure consistency, and trial results were discarded if other vessels came within 1km of the hydrophone. It should be noted however that repeat runs were not conducted for these trials, and the exact bathymetry of the test area is not known. Caution is therefore advised when comparing these results to other published data.

The results, given in figure 9, show an increase in the sound pressure level from 6 to 11 knots, with the overall sound level increasing by approximately 4 dB. Tonal components are clearly visible at both speeds, and the higher frequency broadband contribution is higher at 11 knots, which may indicate cavitation at this speed. The tonal noise is dominated by the engine noise rather than that of the propeller, and this is most apparent for the 11 knot case. Here, the engine speed was approximately 3200rpm, or 53.3Hz, and there is a clear tonal component at 4 times this in figure 9. The tonal components at 6 knots also coincide with multiples of the engine shaft speed. The propeller on the RIB extends below the hull, and so operates in a relatively clean flow when compared to many vessels and this helps to explain why frequencies associated with the propeller blade rate are less dominant.

#### 4 Conclusions and further research

This work has considered noise levels in shallow waters, both in terms of noise from small boats and the propagation of noise through shallow water. Numerical modelling has shown that the propagation is dependent on water depth and the nature of the seabed, and that the propagation losses are generally lower than they are in deep water. The acoustic field created by a single monopole source becomes increasingly complex as the depth reduces, particularly for a hard seabed where most of the incident waves are reflected. This leads to significant spatial variations in the mean acoustic field which should be taken into account when carrying out trials in shallow water.

The hydrophone data has shown that small vessels are significant contributors to noise levels in shallow, coastal waters and this is likely to be having a detrimental impact on marine life. The noise levels are elevated across a broad frequency range, particularly if propellers are cavitating. This increases the detectability of small naval vessels operating in littoral waters, making them vulnerable to attack and reducing their effectiveness. This needs to be given greater attention, especially for those operations that are moving towards the use of larger numbers of small unmanned or autonomous vessels, as these vessels tend to be small and noise levels are often given less attention.

The relationship between speed and noise is complex and relates to the running attitude of the vessel as well as propeller design and engine selection. Whilst the general trend for large commercial vessels is that they produce more noise at higher speeds, this is not always the case for small craft or those operating with controllable-pitch propellers. Engine and propeller selection plays a very important role for small boat noise, particularly those powered by outboard engines. As has been well documented and further demonstrated in the acoustic results in the previous section of this paper, engine noise dominates at lower speeds, with propeller cavitation dominating at higher speeds. For a given propeller design providing a fixed amount of thrust, the larger the diameter the lower the thrust per unit area, and so the lower the propensity for cavitation will be. However, it is often the case that the primary driver for engine and propeller selection is cost, which frequently leads propellers being selected that are too small. More careful engine and propeller selection could therefore have a significant impact on radiated noise levels, but further trials are needed to quantify the potential gains.

Electric propulsion systems have the potential to reduce radiated noise levels significantly, as these remove the noise associated with combustion engines such as tones at multiples of the cylinder firing rates. There are some studies showing the improvements that electric propulsion systems can make (Parsons et al., 2020), but further research is needed across a broader range of vessel types to understand and quantify the potential benefits. Despite the advances in electric propulsion and battery technology, it is envisaged that combustion engines will remain dominant for at least the next decade. Therefore, efforts should still be made on reducing the noise levels from traditional engines, including mounts for both inboard and outboard engines.

### **Acknowledgement**

The Authors would like to thank RS Aqua for their technical support for the Porpoise hydrophone.

### **References**

- Ainslie, M., Dahl, P., De Jong, C., 2014. Practical spreading laws: The snakes and ladders of shallow water acoustics, in: Proceedings of the 2nd International Conference and Exhibition on Underwater Acoustics, pp. 22–27.
- Ainslie, M.A., Martin, S.B., Deveau, T.J., MacGillivray, A.O., Bae, C., Wittekind, D., 2021. Towards a standard for vessel noise measurement in shallow water, in: JASCO Applied Sciences.
- Arveson, P.T., Vendittis, D.J., 2000. Radiated noise characteristics of a modern cargo ship. *The Journal of the Acoustical Society of America* 107, 118–129.
- Cope, S., Hines, E., Bland, R., Davis, J.D., Tougher, B., Zetterlind, V., 2021. Multi-sensor integration for an assessment of underwater radiated noise from common vessels in san francisco bay. *The Journal of the Acoustical Society of America* 149, 2451–2464.
- Dyndo, M., Wiśniewska, D.M., Rojano-Doñate, L., Madsen, P.T., 2015. Harbour porpoises react to low levels of high frequency vessel noise. *Scientific reports* 5, 1–9.
- Erbe, C., Liong, S., Koessler, M.W., Duncan, A.J., Gourlay, T., 2016. Underwater sound of rigid-hulled inflatable boats. *The Journal of the Acoustical Society of America* 139, EL223–EL227.
- Farcas, A., Powell, C.F., Brookes, K.L., Merchant, N.D., 2020. Validated shipping noise maps of the northeast atlantic. *Science of the Total Environment* 735, 139509.
- Halliday, W.D., Pine, M.K., Insley, S.J., 2020. Underwater noise and arctic marine mammals: Review and policy recommendations. *Environmental Reviews* 28, 438–448.
- Hermanssen, L., Mikkelsen, L., Tougaard, J., Beedholm, K., Johnson, M., Madsen, P.T., 2019. Recreational vessels without automatic identification system (ais) dominate anthropogenic noise contributions to a shallow water soundscape. *Scientific Reports* 9, 1–10.
- ITTC, 2017. Underwater noise from ships, full scale measurements, 7.5-04-04-01.
- Lalander, E., Svedendahl, M., Nordström-Larsson, R., Johansson, T., Andersson, M.H., 2021. The underwater soundscape in the port of gothenburg and estimations of the underwater radiated noise from ships, in: FOI, p. 26.
- Larsson, E., Abrahamsson, L., 2003. Helmholtz and parabolic equation solutions to a benchmark problem in ocean acoustics. *The Journal of the Acoustical Society of America* 113, 2446–2454.

- Li, D.Q., Hallander, J., Johansson, T., 2018. Predicting underwater radiated noise of a full scale ship with model testing and numerical methods. *Ocean Engineering* 161, 121–135.
- MacGillivray, A.O., Li, Z., Hannay, D.E., Trounce, K.B., Robinson, O.M., 2019. Slowing deep-sea commercial vessels reduces underwater radiated noise. *The Journal of the Acoustical Society of America* 146, 340–351.
- McKenna, M.F., Ross, D., Wiggins, S.M., Hildebrand, J.A., 2012. Underwater radiated noise from modern commercial ships. *The Journal of the Acoustical Society of America* 131, 92–103.
- Mickle, M.F., Higgs, D.M., 2018. Integrating techniques: a review of the effects of anthropogenic noise on freshwater fish. *Canadian Journal of Fisheries and Aquatic Sciences* 75, 1534–1541.
- Murchy, K.A., Davies, H., Shafer, H., Cox, K., Nikolich, K., Juanes, F., 2019. Impacts of noise on the behavior and physiology of marine invertebrates: A meta-analysis, in: *Proceedings of Meetings on Acoustics 5ENAL*, Acoustical Society of America. p. 040002.
- Nowacek, D.P., Thorne, L.H., Johnston, D.W., Tyack, P.L., 2007. Responses of cetaceans to anthropogenic noise. *Mammal Review* 37, 81–115.
- Parsons, M.J., Duncan, A.J., Parsons, S.K., Erbe, C., 2020. Reducing vessel noise: An example of a solar-electric passenger ferry. *The Journal of the Acoustical Society of America* 147, 3575–3583.
- Putland, R., de Jong, C., Binnerts, B., Farcas, A., Merchant, N., 2022. Multi-site validation of shipping noise maps using field measurements. *Marine Pollution Bulletin* 179, 113733.
- Simpson, S.D., Radford, A.N., Nedelec, S.L., Ferrari, M.C., Chivers, D.P., McCormick, M.I., Meekan, M.G., 2016. Anthropogenic noise increases fish mortality by predation. *Nature Communications* 7, 1–7.
- Smith, T.A., Ventikos, Y., 2022. A hybrid computational aeroacoustic model with application to turbulent flows over foil and bluff bodies. *Journal of Sound and Vibration*, 116773.
- Svendahl, M., Lalander, E., Sigra, P., Östberg, M., 2021. Underwater acoustic signatures from recreational boats - field measurement and guideline.
- Tani, G., Viviani, M., Rizzuto, E., 2015. Model scale investigation of the effect of different speed reduction strategies on cavitating propeller radiated noise, in: *OCEANS 2015-Genova*, IEEE. pp. 1–8.
- Thorne, P.D., 1990. Seabed generation of ambient noise. *The Journal of the Acoustical Society of America* 87, 149–153.
- Tielbürger, D., Finette, S., Wolf, S., 1997. Acoustic propagation through an internal wave field in a shallow water waveguide. *The Journal of the Acoustical Society of America* 101, 789–808.
- Wenz, G.M., 1962. Acoustic ambient noise in the ocean: Spectra and sources. *The Journal of the Acoustical Society of America* 34, 1936–1956.
- Weston, D., 1971. Intensity-range relations in oceanographic acoustics. *Journal of Sound and Vibration* 18, 271–287.
- Wisniewska, D.M., Johnson, M., Teilmann, J., Siebert, U., Galatius, A., Dietz, R., Madsen, P.T., 2018. High rates of vessel noise disrupt foraging in wild harbour porpoises (*phocoena phocoena*). *Proceedings of the Royal Society B: Biological Sciences* 285, 20172314.

## A Numerical modelling of sound propagation

The noise propagation modelling in section 2 was conducted by numerically solving the acoustic wave equations (equations 3 and 4). The equations are solved for the acoustic pressure  $p$  and acoustic velocity  $u_i$ . The modelling assumes a vanishingly small Mach number ( $M_a \ll 1$ ), which is appropriate for underwater acoustics where the speed of sound is much greater than the characteristic flow speeds associated with marine vessels and propellers.

$$\frac{\partial p}{\partial t} + \rho c^2 \frac{\partial u_i}{\partial x_i} = 0 \quad (3)$$

$$\frac{\partial u_j}{\partial t} + \frac{1}{\rho} \frac{\partial p}{\partial x_j} = 0 \quad (4)$$

The density  $\rho$  and speed of sound  $c$  are assigned according to the properties of the water and the seabed. The equations are solved on a two dimensional domain using a finite-volume approach. The spatial discretisation is second-order and uses an exact Riemann solver, which ensures conservation and controls dispersion errors. The time-stepping is carried out using a third-order Runge-Kutta scheme. Details of the numerical methods used are given in (Smith and Ventikos, 2022). The timestep is chosen to ensure that the Courant number is  $C_o \leq 1.0$ .

The source term is modelled as a boundary condition with a time-varying pressure assigned to it according to the following equation:

$$p_{source} = \sum_{i=1}^5 \zeta_i \sin(2\pi f_i t + \psi_i) \quad (5)$$

where  $\zeta_i$  denotes the amplitude and  $\psi_i$  denotes the phase angle of the  $i^{\text{th}}$  frequency component.